Cumhuriyet Science Journal

e-ISSN: 2587-246X
ISSN: 2587-2680

Cumhuriyet Sci. J., 41(4) (2020) 916-928
http://dx.doi.org/10.17776/csj.762184

Spectroscopic properties of vitamin C: A theoretical work

Lana OMER AHMED [1, 3, *], ***Rebaz ANWAR OMER*** [2, 4]

[1] *Koya University, Faculty of Science & Health, Department of Chemistry, Koya KOY45, F.R. IRAQ*

[2] *Koya University, Faculty of Science & Health, Department of Physics, Koya KOY45, F.R. IRAQ*

[3] *Firat University, Faculty of Science, Department of Physics, 23169 Elazig / TURKEY*

[4] *Firat University, Faculty of Science, Department of Chemistry, 23169 Elazig / TURKEY*

Abstract

Vitamin C is an important human micronutrient. It has many vital biological functions in human health. In this research paper, the molecule of vitamin C was optimized and energy band gaps were determined using DFT and HF methods. In computational quantum theory, Density Functional Theory (DFT) and Hartree-Fock (HF) currently play a significant role in physical chemistry spatially. We chose a 6-311+G basis set on the DFT and HF methods to assess our vitamin C molecule. The FT-IR spectra of vitamin C are reported in the current research. The observed vibrational frequencies are assigned and the computational calculations are performed and the corresponding results are displayed. The structure analysis of the present molecule was investigated by NMR (13C NMR & 1H NMR) and UV-Vis spectra. To assess molecular behavior, Mulliken charge distribution, molecular electrostatic potentials (MEP) and Molecular reactivity description were informed to define the activity of the molecule. All calculations were performed using Gaussian 09 packages.

Article info

History:
Received: 01.07.2020
Accepted: 03.12.2020

Keywords:
Vitamin C,
DFT, HF,
Sepectroscopy,
Electrostatic potential.

1. Introduction

Vitamin C also called ascorbic acid, is a vital nutrient within vegetables and fruits [1]. The ascorbic acid is an organic compound that has two chiral carbons and four stereoisomers as displayed in Figure 1. The chemical structure formula of ascorbic acid is C6H8O6 [2]. Unlike animals human body could not synthesize vitamin C, that's why they must be supplied into their diets [3].

Vitamin C is a vital micronutrient for humans [4]. It can act as an antioxidant. When the oxidative stress is raised, the effects of vitamin C could be most prominent under conditions. The activation of phagocytes performed from many infections that release oxidizing agents (reactive oxygen species). These species in the process of deactivation viruses and the killing of bacteria have a vital role [4-6]. Previous researches in animals and humans have shown that vitamin C could protect from the stress affected by cold and hot environments [7-10]. Vitamin C rates in plasma are ten times lesser than in white blood cells, it means the level of vitamin C is very higher in white blood cells that may show the efficient roles of vitamin C in the immune system cells.

Vitamin C has been revealed to affect the functions of replication of viruses, production of interferon, maturation of T-lymphocytes, phagocytes, etc. in the research laboratory [11-15]. Production of such hormones, metabolism of several amino acids, neurotransmitters and vitamins need vitamin C. Moreover, vitamin C helps the liver to clean toxic substances in the system and the blood in fighting infections [16-18]. Vitamin C reduces the damage caused by exposure to UV radiation. This can't act as a sunscreen, since it is unable to absorb UV radiation. But vitamin C's anti-oxidant activity helps prevent UV damage from free radicals [19]. As well as, vitamin C fights all types of viruses. Though the dosage should be extremely high, a low intake amount of vitamin C can save live. For those with low incomes and limited care options this is very significant. For example, in one well-controlled, randomized study, only 200 mg/day of vitamin C administered to the elderly resulted in improved respiratory symptoms in the most seriously ill, hospitalization. Also in the vitamin C category, there were 80 percent fewer deaths [20].

Various analytical techniques are applied in different matrices to assess vitamin C for instance, titrimetric [21], fluorimetric [22], spectrophotometric [23], high-

*Corresponding author. e-*mail address: lana.omer@koyauniversity.org*

performance liquid chromatography [24], enzymatic [25], kinetic [26, 27], Gaussian computational method [28-35].

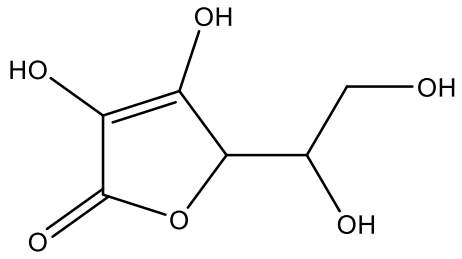

Figure 1: Structure of ascorbic acid.

In this paper, Gaussian program software 09 was performed to determine the Energy Band Gaps, IR, NMR, UV Spectra, Mulliken Charge Distribution, and Molecular electrostatic potential (MEP) maps.

2. Computational Details

Gaussian 09 packages were used to carry out all the calculations. The geometry of the vitamin C molecule has been optimized using (DFT and HF)/6-311+G methods. This basis set produced very accurate results [36, 37]. To investigate all stable structures as optimization energy band gaps, vibrational frequency, Mulliken charge distribution, NMR analysis, UV-Vis spectroscopy, and electrostatic potential map were measured at the same theoretical point.

3. Result and Discussion

3.1 Energy band gaps

The first step of Gaussian program software is to find the optimized molecular structure [38]. Table 1 demonstrated the energy band gaps in electron volt (eV) at 3-21G, 6-31G, 6-31G+, 6-31G++, 6-311G, 6-311G+, cc-pVDZ, LanL2DZ, SDD and DGDZVP with both methods (DFT and HF). As can be seen in the Table 1, the energy band gaps for vitamin C molecule by (Hartree-Fock) HF method have higher values compared with the value of density functional theory (DFT) method. (DFT and HF)/6-311+G methods were chosen for further analysis.

Table 1: The energy band gaps at different basis sets for HF and DFT methods.

Basis sets	HF method Energy gaps (eV)	DFT method Energy gaps (eV)
3-21G	12.71815	5.19578
6-31G	12.59869	5.20993
6-31G+	11.15022	5.21020
6-31G++	10.50721	5.20884
6-311G	12.60577	5.25374
6-311G+	11.13444	5.24558
cc-pVDZ	13.06592	5.51987
LanL2DZ	12.61502	5.19360
SDD	12.62019	5.20421
DGDZVP	13.12116	5.56232

3.2 Molecular construction

Figure 2. revealed the optimized molecular structure of vitamin C with its molecular orientation by DFT and HF on a 6-311+ G basis set. Vitamin C is a weak organic acid that looks like a crystalline and white compound. Structurally, it relates to the six-carbon sugar glucose from which the majority of animals will derive the molecule by a four-step mechanism. Vitamin C is soluble in water, similar to glucose. As can have observed from the mentioned figure, the molecular orientations for DFT and HF method at 6-311+ G basis set have the same orientation.

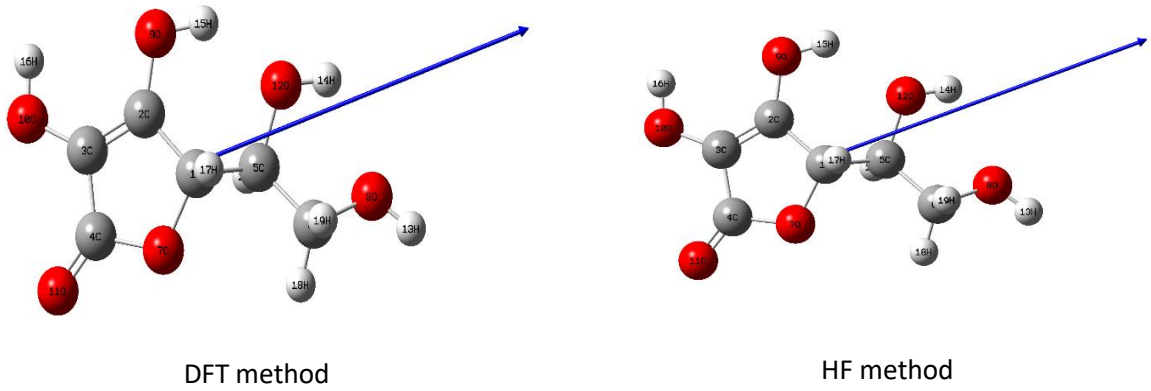

Figure 2: Geometrical structure of vitamin C at 6-311+G basis set.

3.2.1. IR assignments

The vibrational frequency was calculated for vitamin C molecule at (DFT and HF)/6-311+G methods. IR spectra were reported DFT and HF methods respectively with clear vibrations in Table 2. The IR data for both methods are closed to one another but the intensity of the peaks by the DFT method is higher than by the HF method. Below we analyze and list the key functional group in the vitamin C molecule that has been vibrated

.

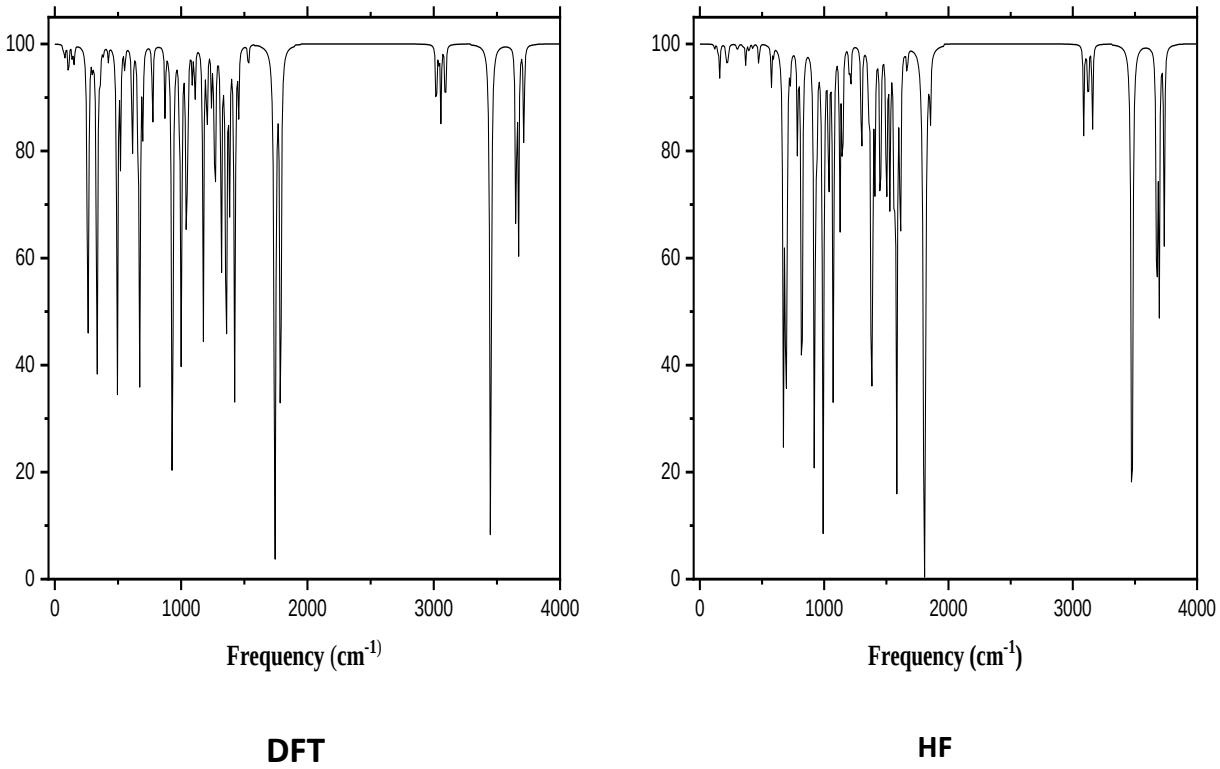

Figure 3. FTIR analysis for Vitamin C by both DFT and HF

Table 2: DFT and HF vibrational frequencies in cm^{-1} with the type of their vibrations

St. NO	Vibrational Assignments	Frequency(cm-1) Observed DFT 6-311+G	St. NO	Vibrational Assignments	Frequency(cm-1) Observed HF 6-311+G
1	(C1-C5)Ro	68.59	1	(C5-C6)Ro	118.11
2	(C5)Ro	81.79	2	(C5)Ro	147.57
3	(O8)Ro	107.72	3	(O8-C6)Ro	159.60
4	(C6)Ro	139.01	4	(C6)Ro	213.03
5	(O9-C2)Sy,St	153.98	5	(C6-H19)Ro	227.02
6	(O9-O10)Sci	246.90	6	(C3-O10)Ro	299.62
7	(O8-H13)Ro	260.87	7	(C3-O10, C2-O9)Sci	308.09
8	(O8-H13)Ro	266.69	8	(C6-H8, C5-O12)Sci	347.99
9	(O10-O11, O12-O8)Sci	298.76	9	(C5-O12, C2-O9)Sci	369.28
10	(C1-O7, C3-C4)Sy,St	315.57	10	(C4=O11, C3-O10)Sci	395.59
11	(O10-H16)Sy,St	333.54	11	(C4-O110Ro	426.60
12	(All Oxygen)Ro	357.15	12	(C6-H19, C1-H17)Ro	474.66
13	(O12, O11)Ro	383.95	13	(C6-H19, C1-H17, C5-H20)Ro	575.01
14	(H19, H14, H17, H20)Ro	423.59	14	(C4=O11)Sy,St	592.99
15	(O12-H14)Ro	494.33	15	(O10-H16)Ro	672.69
16	(C2=C3)St	519.81	16	(O8-H13, O10-H16)Ro	688.40
17	(C3-C4, C2-O9)Sy,St	554.51	17	(O8-H13)Ro	692.83
18	(C1-C2)Sy, St	613.30	18	(C4-O7-C1)Ro	700.12
19	(C3-C4, C2-O9)Sy.St	658.76	19	(C4-O7-C1)Sy, St	728.27
20	(C4-O7-C1)Ro	665.97	20	(O7-C4-C3)Ro	784.83
21	(O9-H15)Ro	672.92	21	(O12-H14)Sy,St	819.42
22	(C3-C4)Ro	697.12	22	(C4-C3-C2)Sy,St	824.25
23	(C4-O7)Sy,St	773.93	23	(O9-H15)Ro	921.72
24	(C2-O2)Sy, St	873.32	24	(C6-H18, C5-H20)Sci	940.27
25	(C4-O7)Sy, St	930.56	25	(C4-O7)Sy,St	991.78
26	(C6-O8)Sy, St	987.52	26	(C4-O7)Sy,St	1036.82
27	(C1-O7)Sy.St	1001.55	27	(C1-O7)Sy,St	1073.28
28	(C3-C4, C1-C5)Sy,St	1038.55	28	(C3-O10)Sy,St	1126.56
29	(C5)Ro	1050.70	29	(C5-H20, C6-H18)Sci	1147.84
30	(C1-C5)Sy,St	1088.15	30	(C6-H19, C1-H17)Ro	1199.18

31	(C1-C5, C3-C4)Sy,St	1109.42	31	(C3-C4)Sy,St	1212.93
32	(O10-H16, C1-H17)Ro	1175.25	32	(O10-H16)Ro	1300.64
33	(H18-H13)Sci	1204.83	33	(H19-C6-H18)Ro	1357.40
34	(C6-H19, C5-H20, C1-H17)Ro	1240.55	34	(C6-H19, C5-H20, C1-H17, O8-H13)Ro	1377.98
35	(C1-H17, C5-H20)Ro	1262.24	35	(C1-H17, O10-H16)Ro	1386.57
36	(C1-H17, C5,H20)Ro	1272.52	36	(C1-H17, C5-H20, O12-H14)Ro	1408.14
37	(C1-C2)Sy, St	1317.92	37	(C1-H17, C5-H20)Ro	1451.75
38	(C1-H17)Ro	1340.85	38	(C1-H17, O12-H14)Ro	1496.29
39	(O9-H15)Ro	1356.64	39	(C5-H20)Ro	1504.73
40	(C5-H20)Ro	1382.75	40	(O10-H16, O9-H15, C5-H20)Ro	1529.32
41	(C3-H16)Sci	1420.74	41	(O10-H16, O9-H15)Ro	1563.62
42	(All hydrogen)Ro	1424.69	42	(H19-C6, H18)Ro	1583.45
43	(C5-C6)Sy,St	1454.92	43	(C5-H20, O12-H14)An, St	1612.72
44	(H19-C6-H18)Sci	1532.23	44	(C6-H19, C6-H18)Sci	1667.35
45	(C3=C2, C4=O11)Sy,St	1742.68	45	(C4=O11, C3=C2)Sy,St	1806.86
46	(C3=C2, C4=O11)Sy,St	1787.18	46	(C3=C2, C4=O11)Sy,St	1853.94
47	(H19-C6-H18)Sy,St	3019.84	47	(H19-C6-H18)Sy,St	3078.59
48	(C1-H17, C5-H20)Sy, St	3038.89	48	(C1-H17, C5-H20)Sy, St	3107.38
49	(C1-H17, C5-H20, C6-H18)Sy, St	3057.03	49	(C1-H17, C5-H20, C6-H18)Sy, St	3124.00
50	(C6-H19,H18)An, Sy	3092.03	50	(C6-H19,H18)An, Sy	3158.19
51	(O9-H15)Sy,St	3449.59	51	(O9-H15)Sy,St	3475.85
52	(O12-H14)Sy,St	3650.78	52	(O12-H14)Sy,St	3676.11
53	(O18-H16)Sy,St	3671.51	53	(O18-H16)Sy,St	3694.76
54	(O8-H13)Sy,St	3713.96	54	(O8-H13)Sy,St	3735.43

Abbreviation: sy: symmetrical, ant: anti-symmetrical, st: stretching, ro: rocking, sci: scissoring

3.2.2. C-C /C=C vibrations

The carbon-carbon vibration within the ring generally occurs in the range of 1400-1600 cm^{-1}[39, 40]. For aromatic vibrations such as the benzene ring, two or more vibrations occur in the benzene ring in the region of 1420-1625 cm^{-1} and the strong vibration starts at 1500 cm^{-1}. The vibration also appears at 1580 cm-1 when the ring is joined to other atoms. In vitamin C the carbon-carbon single bond according to DFT methods vibrated at 1327.92 and 1454.92 cm^{-1}. As well as, the peaks in the range 554.51 – 697.12 cm^{-1} represented to C-C bond. For the HF method, the carbon-carbon single bond appeared at 1212.93 cm^{-1}, also the peaks in the zone 824.25 cm^{-1} represent the vibration of the C-C single bond. The benzene ring in vitamin C has been conjugated to the more groups, this is why the strong vibration for C=C observed at the range 1742.69 – 1787.18 cm^{-1} according to DFT. But by HF methods gives a peak for C=C in a range of 1806.86 – 1853.94 cm^{-1}.

3.2.3. C-H vibrations

The C-H bond is very helpful for identifying the compounds [41]. Due to weak bonds between C-H, typically C-H stretching vibration for aromatic molecule detect in the range 3000-3100 cm^{-1}. The C-H bonding vibration that occurs in the range of 990-1390 cm-1 is in a plane and slows in strength [42, 43]. In the plane above 1200 cm^{-1} the vibration of the carbon-hydrogen interaction appears [44, 45]. The highest vibration of carbon-hydrogen usually observes in the 700-1000 cm^{-1} range [46-48]. In this analysis, for both DFT and HF methods, the peak of C-H vibration out of the plan has been found at 1240.55 – 1272.52 cm^{-1} and 1147.84 – 1199.18 cm^{-1} respectively. Besides, the symmetrical vibration of C-H from the plane was observed at 3010.84 - 3092.03 cm^{-1} this is measured by

DFT. Whereas the C-H symmetric vibration detected at 3078.59 – 3158.19 cm^{-1} using the HF method. The carbon-hydrogen bond in the benzene ring has been vibrated in the range of 1340.85 – 1382.75 cm^{-1} for the DFT method. While it was observed at 1357.40 – 1386.57 cm^{-1} for the HF method. The previous literature fully agrees with these results.

3.2.4. O-H vibrations

The O-H vibration was detected above 3500 cm-1, depending on the region of the OH groups, according to most literature reviews [49-51]. Four hydroxyl groups surround the vitamin C molecule. The OH symmetric vibrated at 3449.59, 3650.78, 3671.51, and 3713.96 cm^{-1} for each O9-H15, O11-H14, O18-H16, and O8-H13 respectively, according to the DFT analysis method, But the peaks were observed at 3475.85, 3676.11, 3694.76, and 3735.43 cm^{-1} for each O9-H15, O11-H14, O18-H16 and O8-H13 by HF analysis method respectively.

3.3. NMR analysis

Researchers use NMR most frequently to investigate the properties of organic molecules, although it applies to any type of sample containing spin nuclei [52-54]. In this study, TMS reference was selected for calculating carbon-NMR and hydrogen-NMR analysis. While for oxygen-NMR the reference is different, H_2O reference has been selected to determine chemical shifts. Chemical shifts of the composite are described in ppm for NMR spectra, as shown in Table 3. The results were quite close to each other for DFT and HF method except for O8 there is a difference in the two values by the two methods. Vitamin C has six carbon atoms, ^{13}C NMR chemical shifts were ordered according to both methods from greater chemical shifts to smaller chemical shifts in ppm unit C4>C2>C3>C5>C1>C6. Eight hydrogens have been combined to construct a vitamin C molecule. As well as, the chemical shifts for ^{1}H NMR were arranged from higher ppm to lower ppm H15>H17>H18>H20>H16>H14> H19>H13. The present molecule has six oxygen. As indicated from the table, the chemical shifts by ^{17}O NMR have appeared at 462.6219, 238.0814, 121.644, 82.4786, 38.3468, and 23.9639 ppm for O11, O7, O9, O10, O12, and O8 respectively at the DFT method. Whereas at HF method have been recorded on 504.8254, 186.97, 78.8812, 45.9034, 11.0545, and -0.699 ppm for O11, O7, O9, O10, O12, and O8 correspondingly.

Table 3: NMR chemical shifts in ppm for vitamin C molecule

Atoms and numbers	DFT on TMS as references	HF on TMS as references
4-C	170.4195	167.8757
2-C	156.8076	146.4632
3-C	124.028	111.8444
5-C	75.9133	53.6446
1-C	71.7333	51.2755
6-C	64.1623	44.2108
	DFT on TMS as references	HF on TMS as references
15-H	6.7316	6.6476
17-H	3.6816	3.1913
18-H	3.4855	3.1658
20-H	3.4047	2.8541
16-H	3.2752	2.8189
14-H	2.9898	2.7745
19-H	2.9514	2.3651
13-H	0.1372	0.0447
	DFT on H_2O as reference	HF on H_2O as reference
11-O	462.6219	504.8254
7-O	238.0814	186.97
9-O	121.644	78.8812
10-O	82.4786	45.9034
12-O	38.3468	11.0545
8-O	23.9639	-0.699

3.4. UV- Vis analysis

UV-Vis spectroscopy is an extremely basic method for chemical composition analysis and complex formation [55]. The time-dependent (TD) for DFT and HF has been used to access UV-Vis spectra to the vitamin C molecule on the basis set 6-311+G. Electron transitions from HOMO to LOMO link to visible absorption maxima. The maximum value of the intensity can refer to these electron transitions at λ max [56]. The λ max value for vitamin C was found at 248.8 nm by the DFT method while it was 198.48 nm by HF method Figure . As can see from the figure, the λ max for both methods quite close to each other but the intensity of λ max in the HF method is higher than in the DFT method.

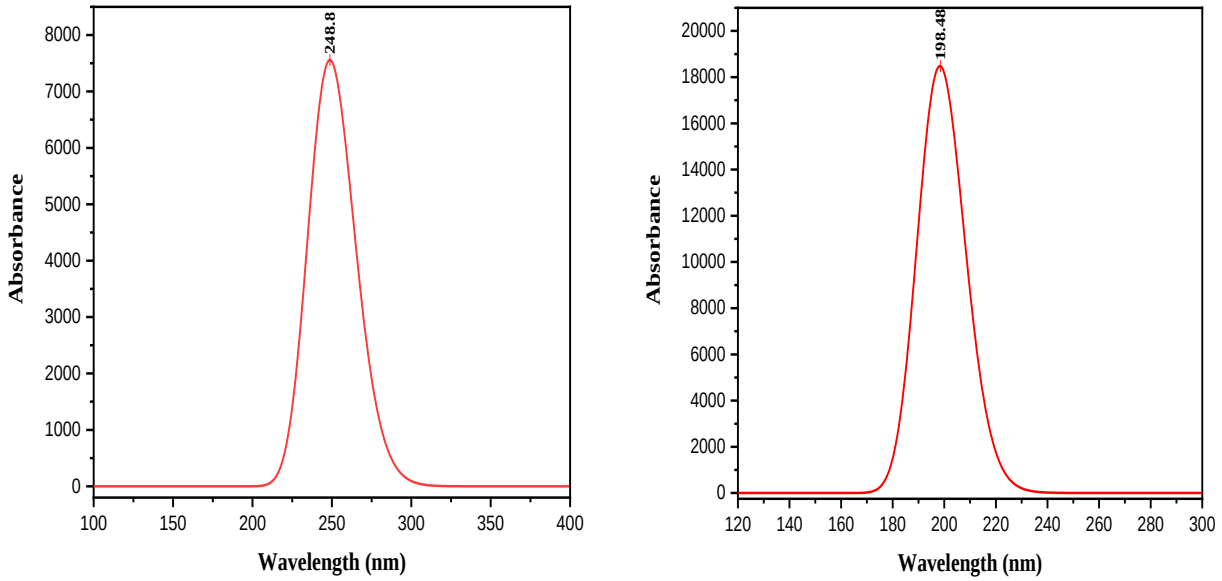

DFT method HF method

Figure 4: UV-visible spectrum for vitamin C

3.5. Mulliken charge

The distribution of the charge on the molecule affects the vibrational spectra significantly [57]. The molecular structure of vitamin C is composed of twenty atoms: six-carbon, six oxygen, and eight hydrogen atoms. Mulliken net charges measured at the level of HF and DFT with an atomic basis set 6-311+G(d, p) in the gas phase using Gaussian 09 Table ***4***. The representation of the plotted atomic charges could be seen in Figure . The table indicated that the HF methods have higher values at the same charges compared to HF methods. As well as, all hydrogen atoms have a positive net charge whereas oxygen atoms have a negative net charge. These atomic charge distribution values on the oxygen of the molecule of vitamin C indicate that the structural part has possible sites for interacting with weak electronic molecules. Vitamin C has six oxygen atoms, that is why it is more reactive with lower electronic molecules. However, carbon atoms have both positive and negative charge distribution. From the plot we can see that C3 is negative by the B3LYP method at the same time it is positive by the HF method.

Table 4: Atomic charges distribution for vitamin C molecule in charge\unit.

No.	Atoms	DFT	HF
1	C	-0.287833	-0.361061
2	C	0.322573	0.458936
3	C	-0.08177	0.054519
4	C	0.314243	0.489259
5	C	0.088844	0.222558
6	C	-0.501136	-0.526243
7	O	-0.183886	-0.321436
8	O	-0.487253	-0.564999
9	O	-0.486624	-0.600861
10	O	-0.483135	-0.623408
11	O	-0.36034	-0.46465
12	O	-0.481535	-0.557593
13	H	0.364765	0.389074
14	H	0.389075	0.427788
15	H	0.411643	0.45086
16	H	0.370781	0.401121
17	H	0.307897	0.327793
18	H	0.258241	0.262899
19	H	0.24288	0.242752
20	H	0.28257	0.292692

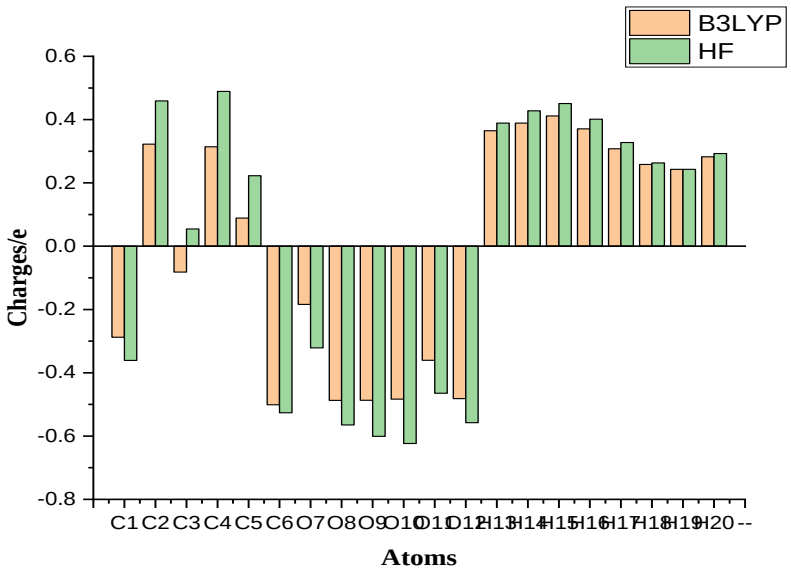

Figure 5: The Mulliken atomic charge plot of vitamin C molecule

3.6. Molecular electrostatic potential (MEP) maps

To Predict reactive electrophilic and nucleophilic attack sites the MEP was determined at the B3LYP and HF/6- 311+G(d, p) for vitamin C molecule. Different colors reflect different values of the electrostatic potential at the surface. The potential increases from red to blue (red < orange < yellow < green < blue). These maps' color code is in the range of -0.07470 a.u. (Extreme red) to 0.07470 a.u. (Deepest blue) using the DFT method. Whereas at the HF method the color cod

of the map is in the range of -0.07998 a.u. (Extreme red) to 0.07998 a.u. (Deepest blue). The MEP for the two mentioned methods is quite similar to each other on the same basis set. MEP's positive (white) regions are correlated to electrophilic reactivity and the negative (red) domains are relevant to nucleophilic reactivity as indicated in

Figure . As shown in the MEP map of the present molecule, the negative regions are based primarily on the oxygen atoms, O11, O7, and O10 atoms. The hydroxyl hydrogen atom locates a maximum positive area showing a potential site for nucleophilic attack. Maximum positive area for H13 located on the H atom bond (belonging to OH group). The MEP map indicates that the negative potential sites are around the electronegative atoms, and also the positive potential sites are across the hydrogen atom. From this article, it can be inferred that the H atoms show the strongest attraction and that the O atom shows the strongest repulsion.

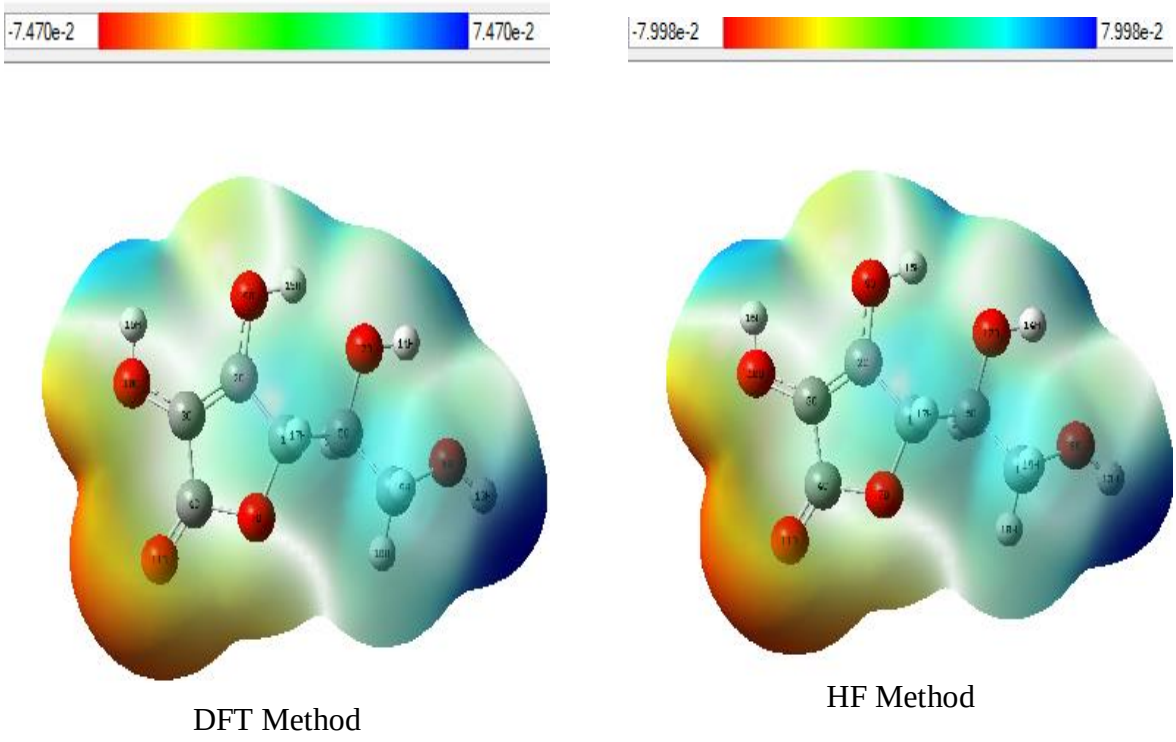

Figure 6: Molecular electrostatic potential (MEP) map for vitamin C molecule

3.7. Molecular reactivity description

Multiple parameters were observed based on the energy level of HOMO and LUMO. The ionization potential ($I=-E_{HOMO}$) is defined as the least amount of energy available to remove an electron from the atom or molecule in the gaseous state. The amount of the discharging energy when one electron added to the gaseous molecule is known as electronic affinity ($A=-E_{LUMO}$). The preference of an atom for attracting electrons is called as electronegativity $\chi= (IP + EA)/2$. In a molecule, weight transfer prevention is denoted by chemical hardness $\eta = (IP-EA)/2$. Other reactivity descriptors, such as chemical potential $\mu= -\chi$, softness $s= 1/2\eta$ and global electrophilicity index $= \mu 2/2\ \eta$, are determined using HOMO and LUMO values [58-60]. Table 5 lists the electronic structure parameter values that were calculated based on the B3LYP/6-311G(dp) technique. The acquisition of extra electronics is concerned with electrophilicity, charging through an electrophile as well as with the opposition put up by the electronic charge exchange device with the environment. An appropriate global descriptor of chemical reactivity is known to be it is not only informative about the transfer of electrons (chemical potential), but also about stability (hardness). The chemical activity of the compound is usually indicated by the HOMO and LUMO energy values and the energy difference between them. A small energy difference between HOMO and LUMO denotes a robust interaction and fast response, while a weak interaction and slow response are denoted by a large

energy difference between HOMO and LUMO [61]. The lower energy gap molecules demonstrate high reactivity and are more polarizable [62, 63]. The arrangement and energy levels of the orbitals, including HOMO and LUMO, determined by the B3LYP/6-311G (dp) level for the current compound, are shown in Figure 7. The results show the higher energy level between HOMO and LUMO equal to 0.19307 eV. All parameters which are indicated the reactivity of the vitamin C are show in Table 5.

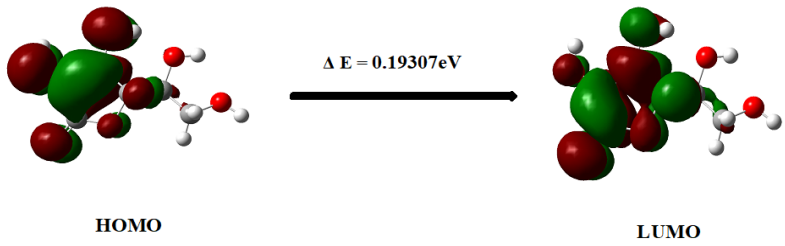

Figure 7: HOMO-LUMO energy bandgap for vitamin C.

Table 5: Electronic parameters for vitamin C.

In a Basis Set B3LYP/6-311G(dp)	Equations	DFT
E LOMO (eV)	E LOMO (eV)	-0.04535
E HOMO (eV)	E HOMO (eV)	-0.23842
Δ E = E HOMO - E LOMO (eV)	HOMO - LOMO	0.19307
I (eV)	I= - EHOMO	0.23842
A (eV)	A= - ELUMO	0.04535
X (eV)	X= I+A/2	0.14188
η (eV)	η = I-A/2	0.04826
S (eV)	S = 1/2n	10.35893
ω (eV)	$\omega = \mu^2/2\eta$	0.20855

4. Conclusions

Both methods (HF and DFT) were investigated in this article to measure vitamin C molecular bandgap energies. 6-311+G basis set has been chosen for the reason it gives precise results. IR shows atomic motions. The illustration of the results culminated in a clear agreement with previous literature. NMR was used to identify the structure of the molecules. In this study, the technique changes (DFT and HF) had very limited effects on the peaks of the atoms. For both methods, all-atom peaks have slowly risen and the number one carbon has a maximum change in a ppm. Additionally, the peaks for both methods (DFT & HF) regularly increase or decrease in ^{1}H NMR. However, the peaks of ^{13}C NMR and ^{17}O NMR have different values using different methods. From the determination of UV-visible spectroscopy, the maximum peaks for vitamin C were detected at 248.8 nm by the DFT method but it was 198.48 nm by the HF method. The Mulliken charge distribution was examined to look at the higher areas of electron density as possible interaction sites, such as oxygen. The electrostatic potential of vitamin C displays that negative regions are associated with O atoms and positive regions are localized on the hydroxyl hydrogen atom. The HOMO-LUMO energy difference for the title compound is 0.19307 eV. The reactivity of the vitamin C was shown with some parameters.

Acknowledgment

Thanks to the head of the physics department (prof. Dr. Niyazi BULUT) Firat University. To learn more thinks about Gaussian.

Conflicts of interest

The authors state that did not have conflict of interests

References

[1] Sehrawat, R., et al., *Technological interventions in the processing of fruits and vegetables*. 2018.

[2] Abbas, S., et al., Ascorbic acid: microencapsulation techniques and trends—a review, *Food Reviews International*, 28 (2012) 343-374.

[3] Iqbal, K., A. Khan, and M. Khattak, Biological significance of ascorbic acid (vitamin C) in human health-a review, *Pakistan Journal of Nutrition*, 3 (2004) 5-13.

[4] Carr, A.C. and S. Maggini, Vitamin C and immune function, *Nutrients*, 9 (2017) 1211.

[5] Segal, A.W., How neutrophils kill microbe,. *Annu. Rev. Immunol.*, 23 (2005) 197-223.

[6] Hemilä, H., Vitamin C and infections, *Nutrients*, 9 (2017) 339.

[7] LeBlanc, J., et al., Studies on acclimatization and on the effect of ascorbic acid in men exposed to cold, *Canadian journal of biochemistry and physiology*, 32 (1954) 407-427.

[8] Dugal, L.P., Vitamin C in relation to cold temperature tolerance, *Annals of the New York Academy of Sciences*, 92 (1961) 307-317.

[9] Strydom, N., et al., Effect of ascorbic acid on rate of heat acclimatization, *Journal of Applied Physiology*, 41 (1976) 202-205.

[10] Chang, C.-Y., et al., Therapeutic treatment with ascorbate rescues mice from heat stroke-induced death by attenuating systemic inflammatory response and hypothalamic neuronal damage,. *Free Radical Biology and Medicine*, 93 (2016) 84-93.

[11] Hemilä, H., Do vitamins C and E affect respiratory infections? (2006).

[12] Hemilä, H., Vitamin C and the common cold, *British Journal of nutrition*, 67 (1992) 3-16.

[13] Beisel, W.R., Single nutrients and immunity., Army Medical Research Inst. of Infectious Diseaes Fort Detrick MD, 1982

[14] Manning, J., et al., Vitamin C promotes maturation of T-cells, *Antioxidants & redox signaling*, 19 (2013) 2054-2067.

[15] Webb, A.L. and E. Villamor, Update: effects of antioxidant and non-antioxidant vitamin supplementation on immune function, *Nutrition reviews*, 65 (2007) 181-217.

[16] Lupulescu, A., Hormones and vitamins in cancer treatment. 1990.

[17] Lupulescu, A., The role of vitamins A, beta-carotene, E and C in cancer cell biology, International Journal for Vitamin and Nutrition Research., 64 (1994) 3-14.

[18] Walingo, K., Role of vitamin C (ascorbic acid) on human health-a review, *African Journal of Food, Agriculture, Nutrition and Development*, 5 (2005).

[19] Devaki, S.J. and R.L. Raveendran, Vitamin C: sources, functions, sensing and analysis, in Vitamin C. 2017.

[20] Saul, A.W., Nutritional treatment of coronavirus. *Orthomolecular Medicine News Service*, 16 (2020) 22.

[21] Verma, K.K., et al., Solid-phase extraction cleanup for determining ascorbic acid and dehydroascorbic acid by titration with 2, 6-dichlorophenolindophenol. *Journal of AOAC international*, 79 (1996) 1236-1243.

[22] Wu, X., et al., Fluorimetric determination of ascorbic acid with o-phenylenediamine, *Talanta*, 59 (2003) 95-99.

[23] Khan, M.R., et al., A simple UV-spectrophotometric method for the determination of vitamin C content in various fruits and vegetables at Sylhet area in Bangladesh, *J. Biol. Sci*, 6 (2006) 388-392.

[24] De Leenheer, A.P. and W. Lambert, Modern chromatographic analysis of vitamins, *Revised and expanded*. 84. 2000.

[25] Casella, L., et al., Rapid enzymatic method for vitamin C assay in fruits and vegetables using peroxidase, *Journal of Food Science*, 54 (1989) 374-375.

[26] Ensafi, A.A., B. Rezaei, and H. Movahedinia, Kinetic–spectrophotometric determination of ascorbic acid by inhibition of the hydrochloric acid–bromate reaction, *Spectrochimica Acta Part A: Molecular and Biomolecular Spectroscopy*, 58 (2002) 2589-2594.

[27] Safavi, A. and L. Fotouhi, Kinetic spectrophotometric determination of ascorbic acid by reduction of toluidine blue, *Talanta*, 41 (1994) 1225-1228.

[28] Ardalan, T., P. Ardalan, and M. Monajjemi, Nano Theoretical Study of a C16 Cluster as a Novel Material for Vitamin C Carrier, *Fullerenes*,

Nanotubes and Carbon Nanostructures, 22 (2014) 687-708.

[29] Harismah, K., et al., Adsorption of vitamin C on a fullerene surface: DFT studies, *Journal of Nanoanalysis*, 4 (2017) 1-7.

[30] Jiang, L., M. Li, and Y. Liu. *Terahertz spectra of vitamins studied by terahertz spectroscopy and density functional theory*. in 26TH International Symposium on Space Terahertz Technology. 2015.

[31] Demianenko, E., et al., A theoretical study on ascorbic acid dissociation in water clusters, *Journal of molecular modeling*, 20 (2014) 2128.

[32] Jiang, L., et al., Terahertz spectra of L-ascorbic acid and thiamine hydrochloride studied by terahertz spectroscopy and density functional theory, *Journal of Infrared, Millimeter, and Terahertz Waves*, 35 (2014) 871-880.

[33] Hou, X., et al., Ascorbic acid induced atrazine degradation, *Journal of hazardous materials*, 327 (2017) 71-78.

[34] Yamabe, S., et al., Frontier orbitals and transition states in the oxidation and degradation of l-ascorbic acid: a DFT study, *Organic & biomolecular chemistry*, 13 (2015) 4002-4015.

[35] Yuan, Y. and R.-N. Zhao, Geometries and stabilities of l-ascorbic acid dimer and its derivatives: a computational investigation by density functional methods, *Journal of the Iranian Chemical Society*, 11 (2014) 863-869.

[36] Wright, J.S., E.R. Johnson, and G.A. DiLabio, Predicting the activity of phenolic antioxidants: theoretical method, analysis of substituent effects, and application to major families of antioxidants, *Journal of the American Chemical Society*, 123 (2001) 1173-1183.

[37] Leopoldini, M., et al., Structure, conformation, and electronic properties of apigenin, luteolin, and taxifolin antioxidants. A first principle theoretical study, *The Journal of Physical Chemistry A*, 108 (2004) 92-96.

[38] Ahmed, L., R. OMER, and H. Kebiroglu, A theoretical study on Dopamine molecule, *Journal of Physical Chemistry and Functional Materials*, 2 66-72.

[39] Tammer, M., G. Sokrates: Infrared and Raman characteristic group frequencies: tables and charts, Springer:2004.

[40] Socrates, G., Infrared and Raman characteristic group frequencies: tables and charts. John Wiley & Sons, 2004:

[41] Wilson, E.B., J.C. Decius, and P.C. Cross, Molecular vibrations: the theory of infrared and Raman vibrational spectra. 1980.

[42] Srivastava, A. and V. Singh, Theoretical and experimental studies of vibrational spectra of naphthalene and its cation. (2007).

[43] Krishnakumar, V. and R.J. Xavier, Normal coordinate analysis of 2-mercapto and 4, 6-dihydroxy-2-mercapto pyrimidines. (2003).

[44] Ramalingam, S., et al., FTIR and FTRaman spectra, assignments, ab initio HF and DFT analysis of 4-nitrotoluene, *Spectrochimica Acta Part A: Molecular and Biomolecular Spectroscopy*, 75 (2010) 1308-1314.

[45] Nagabalasubramanian, P., et al., FTIR and FT Raman spectra, vibrational assignments, ab initio, DFT and normal coordinate analysis of α, α dichlorotoluene, *Spectrochimica Acta Part A: Molecular and Biomolecular Spectroscopy*, 73 (2009) 277-280.

[46] Shoba, D., et al., FT-IR and FT-Raman vibrational analysis, ab initio HF and DFT simulations of isocyanic acid 1-naphthyl ester. Spectrochimica, *Acta Part A: Molecular and Biomolecular Spectroscopy*, 81 (2011) 504-518.

[47] Krishnakumar, V., V. Balachandran, and T. Chithambarathanu, Density functional theory study of the FT-IR spectra of phthalimide and N-bromophthalimide, *Spectrochimica Acta Part A: Molecular and Biomolecular Spectroscopy*, 62 (2005) 918-925.

[48] Nagabalasubramanian, P., S. Periandy, and S. Mohan, Ab initio HF and DFT simulations, FT-IR and FT-Raman vibrational analysis of α-chlorotoluene, *Spectrochimica Acta Part A: Molecular and Biomolecular Spectroscopy*, 77 (2010) 150-159.

[49] Sun, Q., The Raman OH stretching bands of liquid water,. *Vibrational Spectroscopy*, 51 (2009) 213-217.

[50] Zviagina, B.B., et al., Interpretation of infrared spectra of dioctahedral smectites in the region of OH-stretching vibrations, *Clays and Clay Minerals*, 52 (2004) 399-410.

[51] Besson, G. and V. Drits, Refined relationships between chemical composition of dioctahedral fine-grained mica minerals and their infrared

spectra within the OH stretching region. Part I: Identification of the OH stretching bands, *Clays and Clay Minerals*, 45 (1997) 158-169.

[52] Ramalingam, S., et al., Spectroscopic (infrared, Raman, UV and NMR) analysis, Gaussian hybrid computational investigation (MEP maps/HOMO and LUMO) on cyclohexanone oxime,. *Spectrochimica Acta Part A: Molecular and Biomolecular Spectroscopy*, 96 (2012) 207-220.

[53] Kose, E., et al., FT-IR and FT-Raman, NMR and UV spectroscopic investigation and hybrid computational (HF and DFT) analysis on the molecular structure of mesitylene, *Spectrochimica Acta Part A: Molecular and Biomolecular Spectroscopy*, 116 (2013) 622-634.

[54] Karthikeyan, N., et al., Spectroscopic [FT-IR and FT-Raman] and theoretical [UV–Visible and NMR] analysis on α-Methylstyrene by DFT calculations, *Spectrochimica Acta Part A: Molecular and Biomolecular Spectroscopy*, 143 (2015) 107-119.

[55] Zhai, C., et al., Experimental and theoretical study on the hydrogen bonding between dopamine hydrochloride and N, N-dimethyl formamide,. *Spectrochimica Acta Part A: Molecular and Biomolecular Spectroscopy*, 145 (2015) 500-504.

[56] DABBAGH, H.A., et al., UV-vis, NMR and FT-IR spectra of tautomers of vitamin C. Experimental and DFT calculations, *Journal of the Chilean Chemical Society*, 59 (2014) 2588-2594.

[57] OMER, L.A. and O. Rebaz, Computational Study on Paracetamol Drug, *Journal of Physical Chemistry and Functional Materials*, 3 9-13.

[58] Gázquez, J.L., Perspectives on the density functional theory of chemical reactivity, *Journal of the Mexican Chemical Society*, 52 (2008) 3-10.

[59] Rebaz, O., et al., Computational determination the reactivity of salbutamol and propranolol drugs,. *Turkish Computational and Theoretical Chemistry*, 4 67-75.

[60] Calais, J.L., Density-functional theory of atoms and molecules. RG Parr and W. Yang, New York: Oxford University Press, , Oxford, 1989. IX+ 333 pp. Price£ 45.00. *International Journal of Quantum Chemistry*, 47 (1993) 101-101.

[61] Jemmis, E.D., J. Chandrasekhar, and P.v.R. Schleyer, Stabilization of D3h pentacoordinate carbonium ions. Linear three-center-two-electron bonds. Implications for aliphatic electrophilic substitution reactions. *Journal of the American Chemical Society*, 101 (1979) 527-533.

[62] Srivastava, K., et al., Vibrational analysis and chemical activity of paracetamol–oxalic acid cocrystal based on monomer and dimer calculations: DFT and AIM approach, *RSC advances*, 6 (2016) 10024-10037.

[63] Rebaz A. , et al., Theoretical analysis of the reactivity of chloroquine and hydroxychloroquine, *Indian Journal of Chemistry* 59A, (2020) 1828-1834